JJMIE

Volume 16, Number 1, January. 2022
ISSN 1995-6665
Pages 153 - 162

Jordan Journal of Mechanical and Industrial Engineering

Multi-Layer and Multi-Channel Welding Trajectory Control Method of Welding Robot

Baiyang Zhao*

Department of Railway Vehicle, Liaoning Railway Vocational and Technical College, Jinzhou 121000, China

Received 14 July 2021 *Accepted 29 December 2021*

Abstract

In order to solve the problems of low productivity and poor quality stability of manual welding production mode, a multi-layer and multi-channel welding trajectory control method for welding robot is proposed. Firstly, the relationship between the welding current and the forming size of V-groove multi-layer multi pass welding was established by welding process test. At the same time, the starting point of the welding torch can be determined by using the feature point information. In order to verify the feasibility of the above method, V-groove medium and heavy plate workpiece is taken as the test object, and the weld bead is preplanned based on the self-defined filling scheme. The welding parameters are corrected by the above method, and the calculated starting point position of welding gun is compared with the actual welding gun position to verify its accuracy. The results show that the welding parameters of the weld bead can be modified effectively and the position of the welding gun of each pass can be accurately determined by this method, and the error is small. The maximum error of feature point extraction is 9 pixels, and the average error is 5.83 pixels

Keywords: Welding robot; Multi-layer and multi-channel welding; Welding track control.;

1. Introduction

Welding robot have the advantages of a stable welding quality, an improved welding labor productivity, and an improved welding working environment [1]. Since the first emergence of the industrial robot, welding robot has been developed vigorously. Single-side welding robot servo integrated workbench has several advantages, such as convenience, economic structure, compact space, stability and durability. It has significant advantages in ensuring the zero position accuracy of welding gun quality, electrode cap mold, welding quality and so on. It plays an important role in the equipment maintenance process, and has been successfully applied to FANUC robot. However, the current welding robot system is the first generation or quasi second generation robot, only according to the traditional teaching online way to carry out welding work, the trajectory of the welding process can not be well controlled. In the actual welding, there are often deformation, clearance and misalignment. In order to avoid the negative impact of these factors on the quality of the workpiece, the industrial robot is urgently required to have the ability of information feedback and intelligent control. The application of machine vision in industrial robot is a hot spot in robot research. The robot uses a six degree of freedom manipulator to reach the welding point conveniently and flexibly, while avoiding the singularity of its motion trajectory and fully ensuring the stability of the mechanism. Because the precision industrial camera can capture the optical characteristics of the workpiece and reflect it in the CCD lens of the camera, through the visual pattern recognition algorithm based on gray processing, the workpiece can be recognized and located in the gradient direction of edge pixels or geometric elements, so as to realize high-speed visual acquisition, and integrate the functions of image preprocessing, feature extraction and recognition, target positioning, etc., and high hardware processing capacity. Another task is to plan the control strategy of the control system, compile the upper computer software, optimize the multi axis trajectory, and realize the servo control. Finally, a prototype is developed and the verification experiment is carried out. The results show that the welding robot has the characteristics of high stability, high efficiency and high precision when the welding joints are random and the workpiece contour is irregular [2]. The method of quantifying and compensating the path deviation of intersecting curve determined by robot welding path. Weld location is a technical means, which can be used to determine the position of some key points on the intersection curve. The welding sequence has an important influence on the formation of stress and deformation in multi pass welding [3, 4]. At present, most of the artificial sensing navigation methods for service robots focus on the improvement of local path planning and reactive navigation, without considering the global environment. Then, a global path planning method based on pedestrian perception global range and multi-level cost graph is proposed [5]. The robot moves smoothly along the welding path to obtain higher position accuracy. This can be achieved by limiting the motion and dynamic changes of the robot joints, such as joint jitter, acceleration square sum torque when the robot moves along the welding path. In addition, robot walking should be completed in the

* Corresponding author e-mail: zhaobaiyang2020@126.com.

shortest possible time to maintain productivity [6]. Considering the external disturbance and dynamic uncertainty in the process of welding robot trajectory tracking, the controller can effectively suppress the chattering caused by sliding mode control algorithm, effectively realize the trajectory tracking of welding robot, and improve the robustness of the robot [7].

However, the key to solving the above problems is welding robot planning technology, including welding task planning, welding process parameters planning, welding robot path and trajectory planning and control. In this paper, according to the law of the influence of welding process parameters on the weld shape, the functional relationship between the weld cross-section area and wire feeding speed and welding speed is established to realize the welding parameter planning. Through the equal section method, the multi-layer and multi pass welding path planning of double-sided V-groove workpiece is carried out, and the spatial position and posture of welding gun are predicted, and the arrangement law of multi-layer and multi-pass welding of thick plate is established. Then, according to the D-H parameter method, the welding robot model is established in MATLAB, and the welding path is simulated to verify the feasibility of road force planning. Finally, through robot art, the off-line programming software establishes the three-dimensional model of the workpiece and the robot [8], analyzes the spatial position and posture of the welding seam according to the workpiece groove, carries out the trajectory planning and simulation analysis of the workpiece by using the optimization law of the welding process parameters and the multi-layer and multi-channel arrangement law of the thick plate, and then carries out the post-processing of the program, and imports the program into the robot control cabinet to guide the robot to automatically weld the workpiece. Experiments are carried out to verify the feasibility of the program and realize the track control of multi-layer and multi-channel automatic welding of welding robot.

2. Multi-Layer and Multi Pass Welding Path Planning

2.1. Robot motion path

The robot's motion path is composed of target points, and the motion modes between target points are mainly linear interpolation (MOVL), arc interpolation (MOVC) and joint interpolation (MOVJ). The pose information of robot target points recorded by teaching box or offline programming software can be solved by inverse kinematics of robot to calculate the robot joint angles corresponding to different target points [9].

In the process of thick plate multi-layer multi pass welding, there are many welding seams, each welding seam contains multiple paths, and each path contains multiple target points, as shown in Figure 1. The more the target points, the higher the motion accuracy of the robot. However, if there are too many targets, the efficiency will be reduced. If the arc is too long and the amount of filler metal is too much, it will overflow to the base metal, which is easy to cause overflow. The welding sequence of each weld bead in metal welded joints is different, resulting in different residual stresses. The weld is the part piled up or filled with welding materials on the surface or between the base metals. Weld bead refers to the number of specific welds in a layer of weld. If a thin workpiece is welded, only one layer is required, which is a single-layer single pass weld.

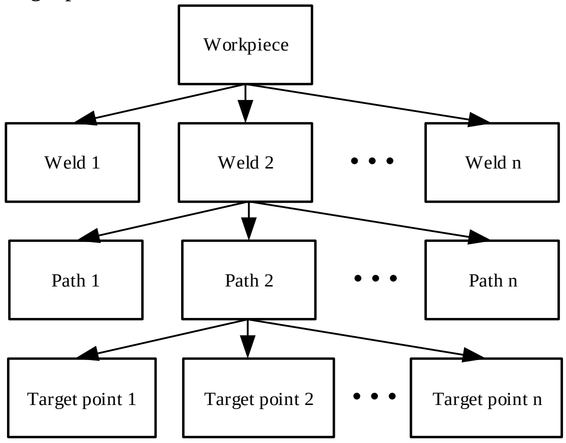

Figure 1. Relationship between weld, path and target point

2.2. Welding parameter planning

When the wire diameter D is constant, the wire feeding speed V1 and welding speed V2 determine the cross-sectional areas of weld bead filling. The equation is as follows:

$$S=\frac{\eta\pi D^2V_1}{4V_2} \tag{1}$$

Among them: η is deposition efficiency. The deposition efficiency η of MAG robot automatic welding used in this paper can reach 90-98%. According to Equation (1), when the welding conditions are determined, the cross-sectional area of weld bead filling can be controlled by adjusting the wire feeding speed and welding speed.

2.3. Weld bead section planning

Asymmetric x-groove is generally used for spherical tank assembly welding, taking V-groove as an example, this paper studies the section planning of multi-layer and multi pass welding path.

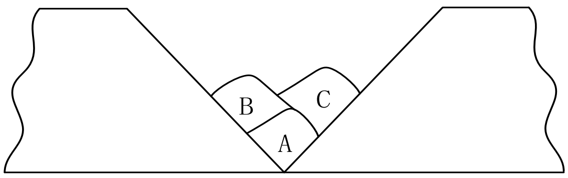

Figure 2. Actual section of V-shaped weld filling

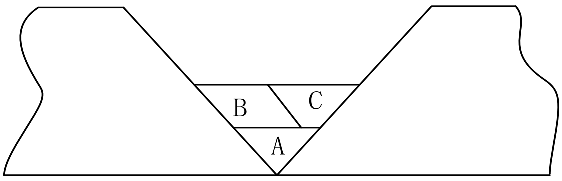

Figure 3. Theoretical section of V-weld filling

Figure 2 shows the actual section of V-shaped weld filling process. The first layer a weld bead is backing weld, which can be approximately triangular. The second layer is composed of two weld passes B and C. The first B weld bead of the second layer can be approximately parallelogram, and the second C weld bead of the second layer can be approximately trapezoidal or triangular.

Figure 3 shows the results of approximate treatment for each pass of V-shaped weld.

When planning the V-groove multi pass welding path, the shape of each groove section perpendicular to the weld bead can be approximately treated as the same, so the position distribution of each weld bead in each section is the same [10]. After simple regularization of the weld bead section shape, the spatial position information of each weld bead in the groove section can be obtained, thus the arrangement rules of multi-layer and multi pass welding can be established [11].

In order to simplify the study, the equal section planning method is adopted in this paper. The cross-sectional area of each weld bead is required to be the same, and the number of passes per layer is also required to be the same as the layer number of the layer.

Assuming that the number of filling layers of V-groove is n, then the total number of passes of filling groove Cn is:

$$C_n = \frac{n(n-1)}{2} + 1 \tag{2}$$

As shown in Figure 4, given the height h and angle θ of groove, the cross-sectional areas of V-groove can be calculated as follows:

$$S = \mathrm{H}_2 \tan\frac{\theta}{2} \tag{3}$$

In the actual welding process, there will be 1-2 mm reinforcement C. According to Equations (2) and (3), the cross-sectional area Sn of the weld bead can be calculated as follows:

$$S_n = \frac{S(2H+C)\tan\frac{\theta}{2}}{C_n} \tag{4}$$

According to Equation (1), when the welding conditions are constant, the wire feeding speed and welding speed can be adjusted by the cross-sectional area of the weld bead.

Set up a coordinate system with point o as the origin, as shown in Figure 4, the upward direction of vertical weldment is z axis, the inward direction of vertical groove section is x axis, and the horizontal right direction is y axis. After regularization of each V-groove section perpendicular to the weld bead, the change of x-axis coordinate value of the target point of the vertical weld bead section can be ignored. Let the height of the first layer of the weld bead is hi, the height of the i-layer is Δ hi, and the coordinates of the corresponding target points PI and j on the j-pass section of the i-layer are (yi, j, zi, J). There are:

$$\Delta h_i = \sqrt{\frac{i(i+1)}{\tan\theta} S_n} \tag{5}$$

$$h_i = \Delta h_i - \sum_{k=1}^{i} h_k \tag{6}$$

According to Equations (5) and (6), the coordinates of the corresponding target points Pi and j on the j-pass section of the i-layer are (yi, j, zi, J):

$$y_{i,j} = y_{i-1,1} - h_i \tan\theta + \frac{(j-1)}{h_i} S_n \tag{7}$$

$$z_{i,j} = z_{i-1,1} + \Delta h_i \tag{8}$$

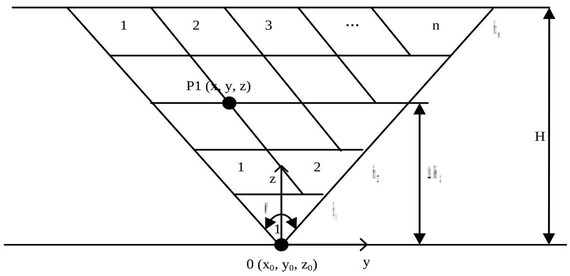

Figure 4. V-groove equal section planning

2.4. Position determination of welding gun

After welding bead layout planning, the position and posture of welding gun should be planned. In order to facilitate welding, the origin of the coordinate system between the weld and the welding gun is usually set as the same. The position of the welding torch is determined by the spatial position of the welding seam Pi, j. the posture of the welding torch needs to be determined according to the geometric characteristics of the weld. In order to prevent the collision between the welding gun and the two sides of the groove, it is necessary to adjust the welding gun posture to ensure that the welding gun is always on the bisector composed of the target point and the groove [12-14].

The coordinate system is established with point o as the origin. The z axis is vertical workpiece upward, x axis is vertical groove section inward, and y axis is horizontal right, as shown in Figure 5. Suppose the deflection angle of welding gun is Δα, and the angle between adjusted welding gun and groove is β. $P_{i,j}$ ($y_{i,j}$, $z_{i,j}$) represents the fixed-point position coordinates of the weld, and H is the groove height. Given the groove height h and angle θ, the relationships (9) and (10) between Δα and β can be established from the geometric relationship of graphs.

$$\tan(\beta - \Delta\alpha) = \frac{H\tan\theta + y_{i,j}}{H - z_{i,j}} \tag{9}$$

$$\tan(\beta + \Delta\alpha) = \frac{H\tan\theta - y_{i,j}}{H - z_{i,j}} \tag{10}$$

From Equations (9) and (10), the deflection angle Δα of welding torch can be calculated as follows:

$$\Delta\alpha = \arctan\left(\frac{H\tan\theta - y_{i,j}}{H - z_{i,j}}\right) - \arctan\left(\frac{H\tan\theta + y_{i,j}}{H - z_{i,j}}\right) \tag{11}$$

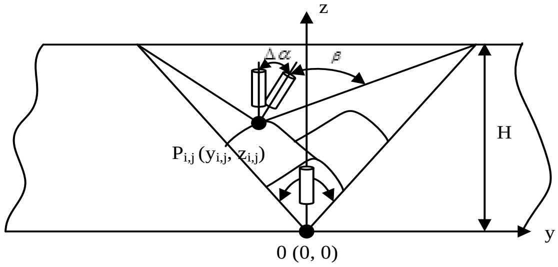

Figure 5. Welding torch posture planning

2.5. Multi pass welding path

In order to improve the welding quality and efficiency, offline programming is used to extract the welding reference path of the workpiece in the multi-layer and multi-pass welding path planning [15-17], and the matrix transformation (translation on the Y-Z plane and deflection transformation around the Z-axis) is performed on the target points on the welding reference path to obtain the pose information of the target points in other welding paths.

It is assumed that the pose matrix of the welding gun at point O is a and that at point Pi and j is B, as shown in Figure 5. From the coordinates of Pi and j and the deflection angle of welding torch Δα, the transformation matrix t of pose matrix A and B can be obtained as follows:

$$\mathbf{T}=\begin{bmatrix} 1 & 0 & 0 & 0 \\ 0 & \cos\Delta\alpha & -\sin\Delta\alpha & y_{i,j} \\ 0 & \sin\Delta\alpha & \cos\Delta\alpha & z_{i,j} \\ 0 & 0 & 0 & 1 \end{bmatrix} \tag{12}$$

$$\mathbf{B}=\mathbf{A}\times\mathbf{T} \tag{13}$$

According to Equation (13), the torch pose matrix B of each weld bead can be obtained by multiplying the torch origin pose matrix A by the transformation matrix T.

2.6. Welding sequence

The welding sequence planning of V-groove is shown in Figure 6, and the number represents the welding sequence [18, 19]. Figure 6(a) shows that each layer is sequentially welded from left to right, and Figure 6(b) shows that each layer is sequentially welded from both sides to the middle.

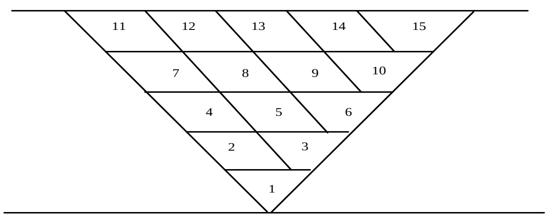

(a) Welding from left to right

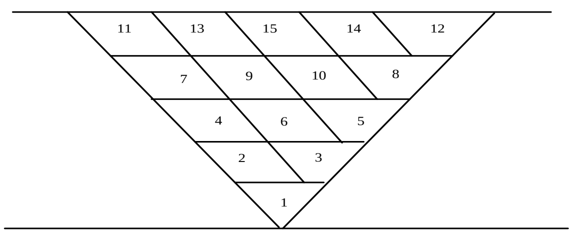

(b) Sequential welding from both sides to the middle

Figure 6 Welding sequence of V-groove

As for the welding layer sequence planning, each welding layer can be sequentially welded from left to right, or each welding layer can be welded alternately, as shown in Figure 7.

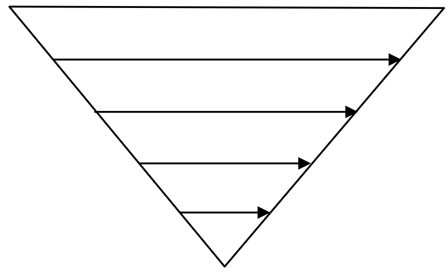

(a) The welding sequence is the same

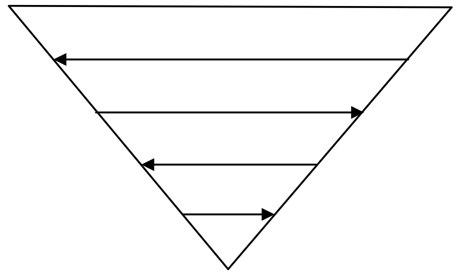

(b) Alternate welding sequence

Figure 7. Schematic diagram of welding layer sequence

In the alternate welding of weld bead and welding layer sequence, due to the imbalance of heat at the arc starting and extinguishing parts of the weld bead, the workpiece deformation is too large and the welding quality is reduced. Therefore, the multi-layer and multi pass welding of spherical tank thick plate is generally selected from left to right welding bead sequence and welding layer sequence welding.

3. Experimental Results

In order to verify the feasibility and accuracy of the multi-layer and multi pass welding adaptive planning method, V-groove workpiece of medium and heavy plate was used for welding test. Firstly, the number of welding passes and welding parameters are preplanned by using self-defined filling strategy and artificial experience. Then, the laser stripe image of each weld bead is collected at the same position. After image processing and feature extraction algorithm, the image feature points are obtained. After coordinate transformation, the actual 3D coordinates under the robot base coordinates are obtained. The actual coordinates of feature points are used to get the width of the weld bead to be filled, and the relationship between the welding parameters and the weld bead forming size is used to modify the preplanning welding parameters. At the same time, the position information of welding torch is calculated by feature point information, and compared with the actual welding torch coordinate point, the error range is analyzed.

3.1. Test conditions and equipment

As shown in Figure 8 which represents the test system diagram, the whole test system is composed of robot system, welding equipment system and laser vision sensing system. The schematic diagram of the test workpiece used is shown in Figure 9. The angle of the bilateral groove of the weld is 90°, the blunt edge is 2 mm, the gap is 2 mm, and the thickness is 16 mm. During the welding process, the welding current and welding torch swing amplitude of each weld bead are different, and the other welding parameters are the same. The number of welding passes and the welding parameters of each weld bead are preplanned by using custom weld bead filling and manual process experience, with a total of 4 layers and 7 passes. The welding process parameters of each weld bead are shown in Table 1. The welding sequence and sequence arrangement of two sides first and then the middle is adopted respectively, as shown in Figure 10.

3.2. Accuracy of image feature extraction

Figure 11 shows the outline of each weld bead groove collected by laser vision sensor. In order to see the groove image of the weld, the original image is rotated to the left by 90° and the coordinate value marked in the figure is the position information of the original image feature points. Table 2 is the coordinates of image feature points obtained by using the related algorithms of image processing and feature extraction in this paper. The coordinates of image feature points are manually marked by drawing software, and compared with the extracted coordinates. The results are shown in Table 2. Therefore, the maximum error of feature points extraction is 9 pixels, and the average error is 5.83 pixels, which can be used for the subsequent coordinate transformation.

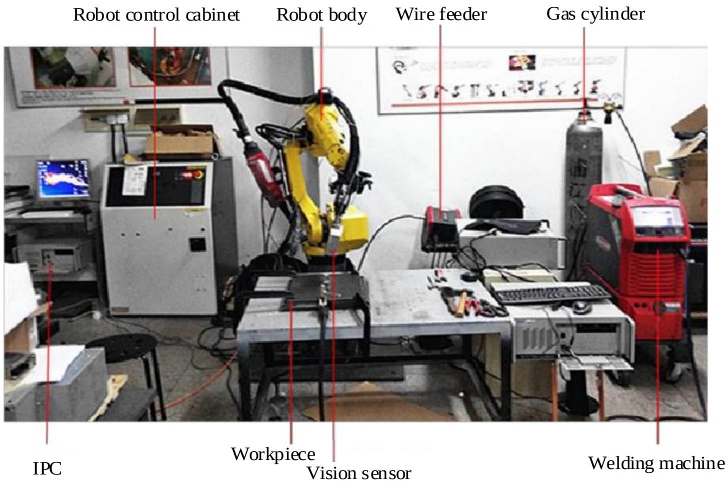

Figure 8. Test system diagram

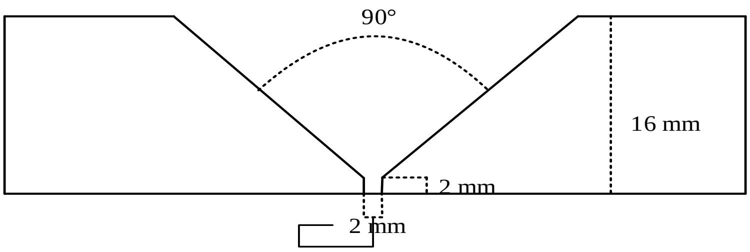

Figure 9. Schematic diagram of test workpiece

Table 1. Welding parameters of each weld bead pre planning

	Current value/A	Swing/mm	Welding speed cm/min	Dip angle/o	Swing frequency/Hz	Left stop/s	Right stop/s
1	180	0	24	0	0	0	0
2	290	4.0	24	0	1.2	0.1	0.1
3.1	220	3.5	24	15	1.2	0.1	0.1
3.2	220	3.5	24	0	1.2	0.1	0.1
4.1	240	4	24	15	1.2	0.1	0.1
4.2	240	4	24	15	1.2	0.1	0.1
4.3	240	4	24	0	1.2	0.1	0.1

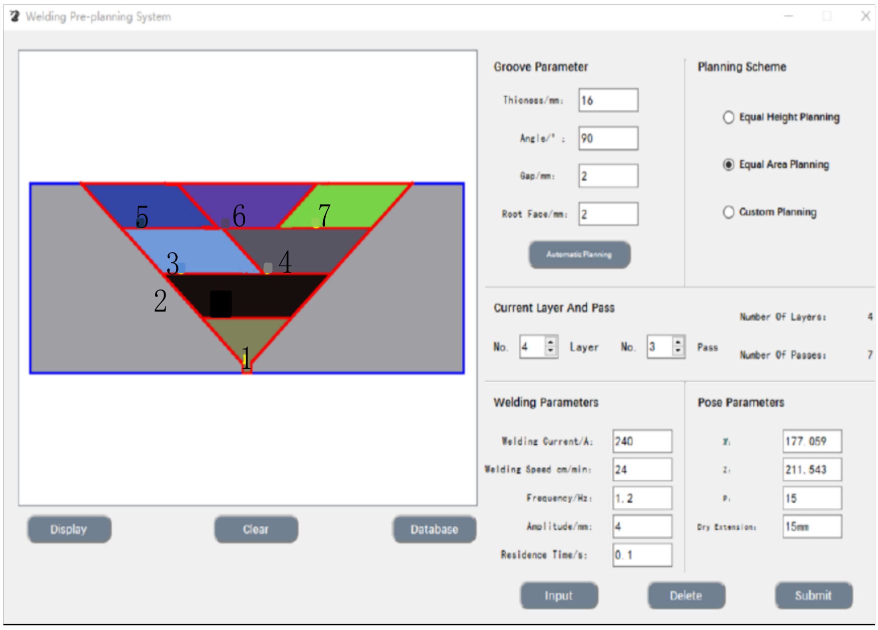

Figure 10. Weld bead layout

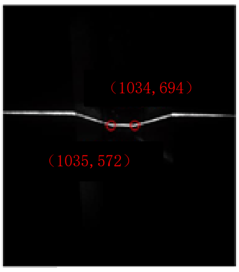

(a) the first line

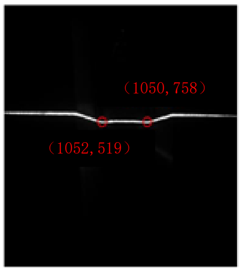

(b) the second way

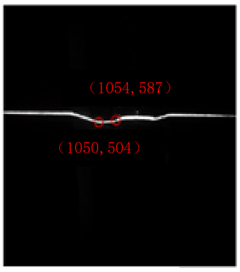

(c) the third way

(d) the fourth line

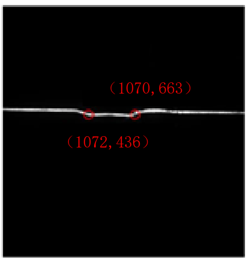

(f) the fifth line

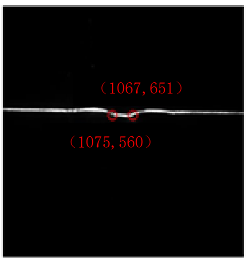

(e) the sixth line

Figure 11. Groove outline and characteristic points after welding

Table 2. Extraction results of image feature points

Number of passes	The first point		Errors/pixels	Second point		Errors/pixels
	Identified image coordinates	Actual coordinates		Identified image coordinates	Actual coordinates	
1	(1035, 572	(1075, 560)	2	(1034, 694)	(1032, 696)	4
2	(1052, 519)	(1054, 517)	4	(1050, 758)	(1055, 755)	8
3.1	(1050, 504)	(1055, 501)	8	(1054, 587)	(1056, 589)	4
3.2	(1072, 442)	(1075, 443)	4	(1067, 818)	(1062, 815)	8
4.1	(1072, 436)	(1074, 431)	7	(1070, 663)	(1076, 666)	9
4.2	(1075, 560)	(1076, 565)	6	(1067, 651)	(1069, 655)	6

3.3. Finished weld

Figure 12 shows the physical picture of each weld bead after welding, and Figure 13 corresponds to the collected weld bead contour map. In order to see the arrangement sequence and the general cross-section shape of the weld bead, the end length of the current weld bead is intentionally shortened by about 2 cm compared with the previous one. It can be seen from Figure 12 that each weld bead is well formed and the workpiece has a good forming appearance after welding. This is because this method performs matrix transformation on the target points on the welding reference path, and adjusts the welding gun attitude to prevent the collision between the welding gun and both sides of the groove.

(a) backing weld (b) the second way (c) the third way (d) the fourth line

(e) the fifth line (f) the sixth line (g) the seventh line

Figure 12. Physical picture after welding

As can be seen from Figure 14, According to Equation (2), if the number of filling layers of V-groove is 4, the total number of filling passes of V-groove is 7. The welding sequence of each weld is 4 layers and 7 passes. At the same time, through Equation (5), Equation (6) and Equation (12). The laser profile of each weld section is converted into coordinates, and the three-dimensional coordinates of the actual laser stripe points are calculated. The coordinates of Y-axis and Z-axis are represented by coordinate diagram, as shown in Figure 15, the actual restoration map of weld cross-section can be obtained. It can be concluded that in the actual welding, the shape of weld bead is irregular, we can simplify it in theory, but in the actual situation, we should use the characteristic points of weld bead to make corresponding correction measures according to different purposes.

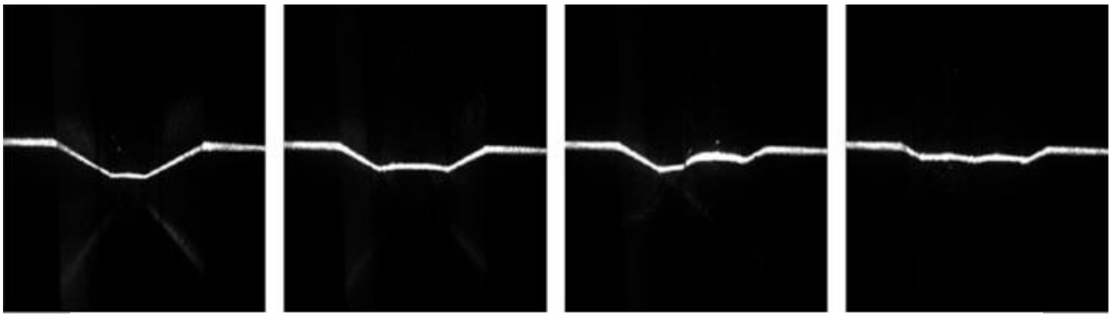

(a) backing weld (b) the second way (c) the third way (d) the fourth line

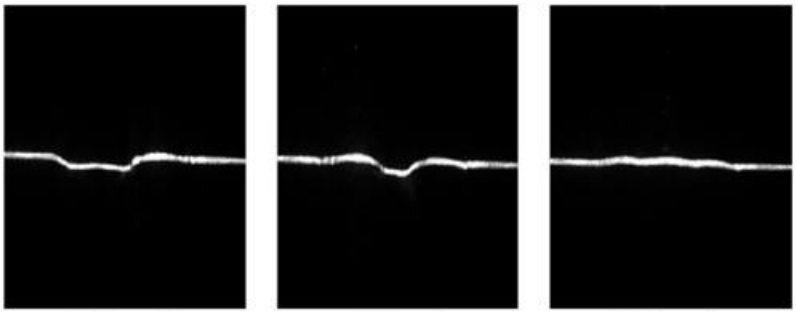

(e) the fifth lane (f) the sixth lane (g) the seventh line

Figure 13. Laser outline of each pass

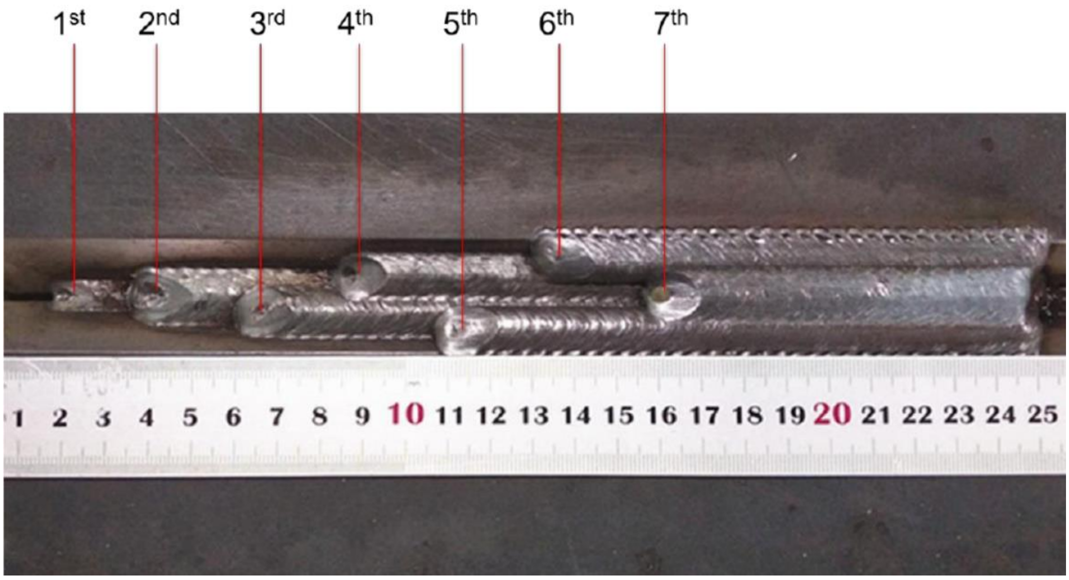

Figure 14. Final physical picture after welding

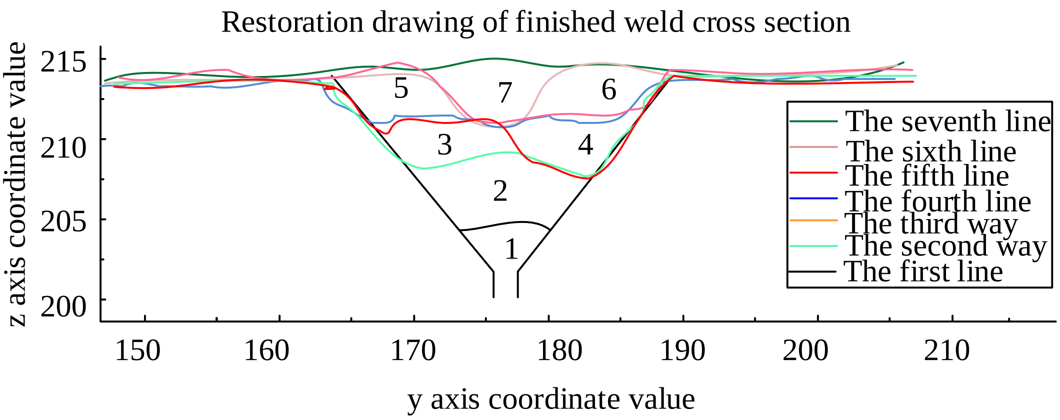

Figure 15. Weld bead section restoration

According to the test results, the filling effect of multi-layer and multi pass welding is basically the same as the planning result. The cross-sectional area of each weld bead is uniform and the welding parameters are not changed too much. It overcomes the problems of low production efficiency and poor-quality stability under the manual welding production mode of the existing welding robot, and improves the welding quality and makes the workpiece have a good forming appearance after welding. This is because that this method adopts the equal section planning method to simplify the research of weld section planning. The off-line programming method is used to extract the welding reference path of workpiece in multi-layer and multi pass welding path planning which improves welding quality and efficiency.

4. Conclusion

In this paper, the multi-layer and multi-channel welding process and trajectory of robot are studied. The results show that the planning path is basically accurate, which can effectively modify the welding parameters of the weld, and accurately determine the position of each welding gun. The results also show that the error is small, and that the multi-layer and multi-pass welding path basically achieves the expected effect.

1. With the welding process, the cross section of the weld bead is closer to the parallelogram.
2. The bottom diamond weld bead welding needs to reduce the welding angle properly to avoid wall collision.
3. Each weld is well formed, and the workpiece has a good forming appearance after welding. It overcomes the problems of low production efficiency and poor quality stability in the manual welding production mode of the existing welding robot.

Acknowledgement

The research is supported by: Scientific Research Project with Funding from Liaoning Education Department (No. LJKY2020113).

References

[1] Wei, J.Y. A servo unilateral spot welding robot integrated workbench. Equipment Manufacturing Technology, 2018, (4): 108-111.

[2] Hendriko, H. Development of invers kinematic method for 6-dof parallel robot using analytical approach. Procedia Manufacturing, 2019, 38: 203-208.

[3] Yan, L.; Jiang, L.; Tian, X.C. An approach to the path planning of intersecting pipes weld seam with the welding robot based on non-ideal models. Robotics and Computer-Integrated Manufacturing, 2019, 55PA: 96-108.

[4] Gao, Q.; Zhan, X.; Shen, H.; Ling, W.; Bu, H. Effect of welding sequence on stress and deformation field of Invar alloy multi-layer and multi-pass welding: A simulation study. Modern Physics Letters B, 2020, (4): 2050129.

[5] Fang, F.; Shi, M.; Qian, K.; Zhou, B.; Gan, Y. A human-aware navigation method for social robot based on multi-layer cost map. International Journal of Intelligent Robotics and Applications, 2020, 4(3): 308-318.

[6] Rout, A.; Bbvl, D.; Biswal, B.B. Optimal trajectory generation of an industrial welding robot with kinematic and dynamic constraints. Industrial Robot: The International Journal of Robotics Research and Application, 2019, 47(1): 68-75.

[7] Wang, P.; Zhang, D.; Lu, B. Robust fuzzy sliding mode control based on low pass filter for the welding robot with dynamic uncertainty. Industrial Robot, 2020, 47(1): 111-120.

[8] Zhang, X.H. Teaching design of ABB robot palletizing workstation based on Robot Art. Electronic Test, 2019, (22): 112-114.

[9] Jiang, L.; Zhu, Z.; Liu, H.; Zhu, J. Analysis of dynamic characteristics of water hydraulic rotating angle self-servo robot joint actuator. Journal of Intelligent & Robotic Systems, 2018, 92(2): 279-291.

[10] Ginzburg, S.; Morozova, L.; Kloshek, A.; Ossenbrink, R.; Michailov, V.; Bobrynina, E.; Koltsova, T.; Tolochko, O.; Kocak, M.; OEzbek, S. Addition of nanoparticles to flux cored wires for the nucleation of acicular ferrite micro-structure in weld metals of the high-strength low-alloy steel. Welding and Cutting, 2020, 19(1): 48-53.

[11] Cho, D.W. Algorithms of mathematical models for fast multi-pass weld-bead drawing technique in V-groove welding. Journal of Mechanical Ence and Technology, 2019, 33(11): 5347-5352.

[12] Masoud, Z.; Nazzal, M.; Alhazza, K. Multimode input shaping control of flexible robotic manipulators using frequency-modulation. Jordan Journal of Mechanical and Industrial Engineering, 2016, 10(3): 179-188.

[13] Liu, Y.; Shi, L.; Tian, X. Weld seam fitting and welding torch trajectory planning based on NURBS in intersecting curve welding. International Journal of Advanced Manufacturing Technology, 2018, 95(1-4): 2457-2471.

[14] Shen, Z.B.; Zhang, X.X.; Zhang, B.; Wu, X.Q.; Zhu, X.G. Application of multi-function welding torch fixture in welding robot. Science & Technology Vision, 2019, (8): 144-145.

[15] Wei, A.G.; Chang, B.H.; Xue, B.C.; Peng, G.D.; Du, D.; Han, Z.D. Research on the Weld Position Detection Method for Sandwich Structures from Face-Panel Side Based on Backscattered X-ray. Sensors, 2019, 19(14): 3198.

[16] Dildin, A.N.; Gerasimov, V.Y.; Zaitseva, O.V. The structure of multi-layer composite material obtained by the method of diffusion welding. Materials Science Forum, 2019, 946: 139-144.

[17] Agarwal, S.; Chakraborty, S.; Prasad, K.; Chakraborty, S. A rough multi-attributive border approximation area comparison approach for arc welding robot selection. Jordan Journal of Mechanical and Industrial Engineering, 2021, 15(2): 169-180.

[18] Wei, W.; Yun, C.; Song, D.; Wang, W. Path planning for robotic multi-path/multi-layer welding. Jiqiren/Robot, 2014, 36: 257-262+270.

[19] Shan, Z.; Xu, X.; Tao, Y.; Xiong, H. A trajectory planning and simulation method for welding robot. 2017 IEEE 7th Annual International Conference on CYBER Technology in Automation, Control, and Intelligent Systems (CYBER), 2017, 510-515.